

Reservoir Description By Using a Piecewise Constant Level Set Method*

Hongwei Li

Center for Integrated Petroleum Research, University of Bergen, Norway, and Department of Mathematics, Capital Normal University, China. Hongwei.li@cipr.uib.no

Xue-Cheng Tai

Department of Mathematics, University of Bergen, Norway, and Division of Mathematical Sciences, School of Physical and Mathematical Sciences, Nanyang Technological University, Singapore.

Tai@mi.uib.no

Sigurd Ivar Aanonsen

Center for Integrated Petroleum Research, University of Bergen, Norway, and Department of Mathematics, University of Bergen, Norway. Sigurd.Aanonsen@cipr.uib.no

Dedicated to Prof. Cui Junzhi on the occasion of his 70th birthday.

Abstract

We consider the permeability estimation problem in two-phase porous media flow. We try to identify the permeability field by utilizing both the production data from wells as well as inverted seismic data. The permeability field is assumed to be piecewise constant, or can be approximated well by a piecewise constant function. A variant of the level set method, called Piecewise Constant Level Set Method is used to represent the interfaces between the regions with different permeability levels. The inverse problem is solved by minimizing a functional, and TV norm regularization is used to deal with the ill-posedness. We also use the operator-splitting technique to decompose the constraint term from the fidelity term. This gives us more flexibility to deal with the constraint and helps to stabilize the algorithm.

Mathematics subject classification: 34A55, 35R30.

Key words: inverse problem, level set method, piecewise constant, operator splitting, reservoir description.

1. Introduction

History matching, i.e, the process of tuning uncertain properties to match dynamic data is an important part of reservoir flow modelling. The flow in the reservoir (porous medium) can be modelled by multiphase flow equations. If the physical (rock) properties of the reservoir, such as porosity, permeability etc. are known, then we can predict the pressure and saturation distributions by solving the flow equations. However, such information usually are only available at wells. On the other hand, the production data from wells, as well as seismic data might be available, which can provide sparsely distributed pressure and saturation information. Based on these data, we should be able to get some information about the rock properties. However, because of the sparsity of data, one shouldn't expect to identify the fine details. We focus on permeability estimation in this paper, and all the other rock properties, such as porosity, viscosity etc, are supposed to be known.

* Received xxx / Revised version received xxx /

Permeability estimation is an inverse problem, which is ill-posed and usually needs regularization. In our case, the ill-posedness is worse because of the insufficient observation data. To overcome this difficulty, we give up pursuing the fine resolution of the permeability field, and adopt the common used zonation regularization strategy. To do so, the parameter field is assumed to be piecewise constant. This reduces the solution space, so that non-feasible solutions should be avoided. Accordingly, TV (Total Variation) norm regularization will be used to control the shape of the curves separating different constant permeability regions, which has the ability to preserve sharp interfaces [1].

When solving curve evolution problems, the level set method is a natural choice, because of its excellent ability to deal with topological changes, such as breakings or mergings, in a natural and efficient way. Since the permeability estimation problem considered here involves identifying the curves separating different regions, we will also use level set method to represent the interfaces implicitly, and solve the inverse problem by evolving the level set functions.

The original level set method was proposed by Osher and Sethian in [2]. Recently, the level set method has been extended and used for various inverse problems [3, 4, 5, 6, 7]. Recently, some variants of the Osher-Sethian level set method have been proposed [8, 9]. A variant of level set method, called binary level set method, was proposed in [10, 9] and used for image processing. It simplifies the original level set method, and may gain some advantages for certain problems. This method has been tested for our problem for the case that the permeability field consists of two regions of constant values, see Nielsen et. al. [11]. By binary level set method, the zonation structure is implicitly represented by binary level set functions. One binary level set function can represent two regions. With more than two regions, we need to use multiple binary level set functions, see [12, 8]. This is just the multiple (traditional) level set method framework, proposed by Chan et.al. [13, 14]. The piecewise constant level set method [8], is another variant of the level set method. However, piecewise constant level set method has the ability to deal with multiple regions using just one level set function. This is simpler than the multiple binary level set method.

In this paper, we try to identify the permeability field with zonation structure by using the piecewise constant level set method of [8]. The permeability field is assumed to be piecewise constant, or can be approximated well by piecewise constant functions. The observation data available is production data from wells and inverted, time-lapse seismic data.

The remainder of this paper is organized as follows. In Section 2, the inverse problem and corresponding minimization problem are set up. In Section 3, the piecewise constant level set method is introduced and incorporated into the formulation of the minimization problem. The numerical algorithm is described in Section 4. Numerical experiments are presented in Section 5. Section 6 is for conclusion and remarks.

2. The inverse and minimization problem

We consider incompressible, two dimensional two phase flow (oil and water) in a porous medium with isotropic permeability and zero capillary pressure.

$$\Phi(x) \frac{\partial S_o}{\partial t} - \nabla \cdot \left(\frac{\kappa(x) \kappa_{ro}(S_o)}{\mu_o} \nabla p \right) = f_o(x), \quad (2.1)$$

$$\Phi(x) \frac{\partial S_w}{\partial t} - \nabla \cdot \left(\frac{\kappa(x) \kappa_{rw}(S_w)}{\mu_w} \nabla p \right) = f_w(x), \quad (2.2)$$

where $(x, t) \in \Omega \times [0, T]$. $\Omega \in \mathbb{R}^2$ is a bound domain. The subscripts o and w refer to oil and water. S_o, S_w denote the saturations, μ_o, μ_w denote the viscosity, p denotes the pressure, f_o, f_w denote the external volumetric flow rate and κ_{ro}, κ_{rw} denote the relative permeability. $\Phi(x)$ is the porosity, and $\kappa(x)$ denotes the absolute permeability, which is to be identified in this paper.

Using the auxiliary equation

$$S_o + S_w = 1 \quad (2.3)$$

to eliminate the oil saturation, S_o , we obtain a system of two equations in the two unknowns, pressure p and water saturation S_w .

The problem is to estimate the absolute permeability $\kappa(x)$, while $\Phi(x)$ and κ_{ro}, κ_{rw} are assumed to be known. The estimation is based on the observation data from production history of wells as well as the data from seismic surveys.

Incorporating seismic data into history matching is relatively new. Although some researchers use seismic amplitude differences[15], most of the work on seismic history matching has been focusing on inverted seismic data, such as acoustic impedance and/or Poisson's ratio, see e.g. [16, 17, 18, 19]. These properties are mapped to the simulation grid and compared to corresponding properties calculated from the model porosity and simulated pressures and saturations using a petro-elastic model. In this paper, we have, for simplicity, assumed that both the production data and the seismic data has been inverted to cell pressures and saturations. Converting time-lapse seismic data to changes in pressures and saturations is a difficult task, which is currently not normally done. However, this is the topic of ongoing research, see e.g., [20, 21, 22, 23].

Let d_{well} and d_{seis} denote the well data and seismic survey data respectively, i.e.

$$\begin{aligned} \mathbf{d}_{well} &= \{p(x_{well,i}, t), S_w(x_{well,i}, t), \quad i = 1, 2, \dots, n_{well}, t \in [0, T]\}, \\ \mathbf{d}_{seis} &= \{p(x, t_j), S_w(x, t_j), \quad x \in \Omega, j = 1, 2, \dots, n_{seis}, \end{aligned}$$

where n_{well} is the number of wells including both production wells and injection wells, and n_{seis} is the number of seismic surveys in the time domain $[0, T]$.

Given the absolute permeability field, we can compute p, S_w and then measure the differences between the observed data and the simulated data. In this paper, we will formulate this process as an output-least-squares optimization problem, and then solve it by a variational approach.

Based on the standard technique, we would like to identify the logarithm of the permeability rather than the permeability itself. So we define

$$q(x) = \log_{10}(\kappa(x)),$$

where the permeability, $\kappa(x)$, is given in Darcys, and solve the problem with respect to $q(x)$."

As in [18, 19], we apply the following objective function to measure the misfit between the measured and simulated data.

$$\begin{aligned} J(q) = J_{tot}(q) &= J_{well}(q) + J_{seis}(q) \\ &= \frac{1}{2}(\mathbf{d}_{well} - \mathbf{m}(q))^T D_{well}^{-1}(\mathbf{d}_{well} - \mathbf{m}_{well}(q)) + \\ &\quad \frac{1}{2}(\mathbf{d}_{seis} - \mathbf{m}(q))^T D_{seis}^{-1}(\mathbf{d}_{seis} - \mathbf{m}_{seis}(q)), \end{aligned} \quad (2.4)$$

where $\mathbf{m}_{well}(q)$ and $\mathbf{m}_{seis}(q)$ are the simulated data from solving the forward model for a given $q(x)$. D_{well} and D_{seis} are the covariance matrices corresponding to data error.

We consider the special case that $q(x)$ is a piecewise constant function or can be well approximated by a piecewise constant function. While arbitrary geometrical structures are allowed, the interfaces should not be too arbitrary to be out of the ordinary world. We need to control the local behavior of the interfaces. This is achieved by TV norm regularization. Define

$$R(q) = \int_{\Omega} |\nabla q| dx.$$

Then the functional to be minimized is

$$F(q) = J_{tot}(q) + \beta R(q), \quad (2.5)$$

where $\beta > 0$ is the regularization parameter to be used to control the influence of the regularization. We choose β by trial and error method in this paper. Now the problem is

$$\min_{q \in Q} F(q), \quad (2.6)$$

where Q is the space containing all piecewise constant functions.

In the next section, we try to utilize the fact that q lies in a piecewise constant function space, and represent q by a piecewise constant level set function. By doing this, the structure of q , i.e. the location of discontinuities and the constant values (levels) can be recovered simultaneously.

3. The Piecewise Constant Level Set Method for the inverse problem

We use the PCLSM [8] to represent q as well as its discontinuities implicitly. The essential idea of the PCLSM is to use a piecewise constant level set function to identify the subdomains. Assume that we need to partition the domain Ω into subdomains Ω_i , $i = 1, 2, \dots, n$ and the number of subdomains n is a priori known. In order to identify the subdomains, we try to identify a piecewise constant level set function ϕ such that

$$\phi = i, \quad \text{in } \Omega_i, \quad i = 1, 2, \dots, n. \quad (3.1)$$

Thus, for any given partition $\{\Omega_i\}_{i=1}^n$ of the domain Ω , it corresponds to a PCLS function ϕ which takes the values $1, 2, \dots, n$. Associated with such a level set function ϕ , the characteristic functions of the subdomains are given as

$$\psi_i = \frac{1}{\alpha_i} \prod_{j=1, j \neq i}^n (\phi - j), \quad \alpha_i = \prod_{k=1, k \neq i}^n (i - k). \quad (3.2)$$

If ϕ is given as in (3.1), then we have $\psi_i(x) = 1$ for $x \in \Omega_i$, and $\psi_i(x) = 0$ elsewhere. We can use the characteristic functions to extract geometrical information for the subdomains and the interfaces between the subdomains. For example,

$$\text{Length}(\partial\Omega_i) = \int_{\Omega} |\nabla \psi_i| dx, \quad \text{Area}(\Omega_i) = \int_{\Omega} \psi_i dx. \quad (3.3)$$

Define

$$K(\phi) = (\phi - 1)(\phi - 2) \cdots (\phi - n) = \prod_{i=1}^n (\phi - i). \quad (3.4)$$

At every point in Ω , the level set function ϕ should satisfy

$$K(\phi) = 0. \quad (3.5)$$

For any piecewise constant function $q(x)$, we can represent $q(x)$ by a piecewise constant level set function described above. Suppose $q(x)$ is defined in domain $\Omega = \bigcup_{i=1}^n \Omega_i$, and $q(x) = c_i$, $x \in \Omega_i$. Assume that a piecewise constant level set function $\phi(x)$ has been defined as $\phi(x) = i$, $x \in \Omega_i$, then we have

$$q(x) = q(\vec{c}, \phi)(x) = \sum_i^n c_i \psi_i(\phi),$$

where $\vec{c} = (c_1, c_2, \dots, c_n)^T$. Incorporating above representation, together with the constraint, the minimization problem (2.6) becomes

$$\min_{\vec{c}, \phi} F(q(\vec{c}, \phi)), \quad \text{subject to } K(\phi) = 0. \quad (3.6)$$

To deal with the constraint, we use the penalization technique to transform the constrained minimization problem (3.6) into an unconstrained minimization problem

$$\min_{\vec{c}, \phi} L(q(\vec{c}, \phi)), \quad L(q(\vec{c}, \phi)) = F(q(\vec{c}, \phi)) + \frac{1}{2\mu} \int_{\Omega} |K(\phi)|^2 dx, \quad (3.7)$$

where μ should be a small positive number to enforce $K(\phi) = 0$.

To solve the above minimization problem, we need to calculate the derivatives of F with respect to ϕ and \vec{c} . By the chain rule, we have [12]

$$\frac{\partial F}{\partial \phi} = \frac{\partial F}{\partial q} \frac{\partial q}{\partial \phi} \quad (3.8)$$

$$\frac{\partial F}{\partial c_j} = \int_{\Omega} \frac{\partial F}{\partial q} \frac{\partial q}{\partial c_j}, \quad \forall j = 1, 2, \dots, n. \quad (3.9)$$

The calculation of $\frac{\partial F}{\partial q}$ involves the solving of the forward model. In this work, $\frac{\partial F}{\partial q}$ is calculated from the adjoint state variables, see e.g., [24].

4. The numerical algorithm

For simplicity, we Let $L(\vec{c}, \phi) = L(q(\vec{c}, \phi))$, $F(\vec{c}, \phi) = F(q(\vec{c}, \phi))$. So the functional to be minimized is

$$L(\vec{c}, \phi) = F(\vec{c}, \phi) + \frac{1}{2\mu} W(\phi), \quad (4.1)$$

where $W(\phi) = \int_{\Omega} K^2(\phi) dx$. It's easy to see that

$$\frac{\partial L}{\partial \phi} = \frac{\partial F}{\partial \phi} + \frac{1}{2\mu} W'(\phi), \quad (4.2)$$

$$\frac{\partial L}{\partial \vec{c}} = \frac{\partial F}{\partial \vec{c}}, \quad (4.3)$$

where $\frac{\partial L}{\partial \vec{c}} = (\frac{\partial L}{\partial c_1}, \frac{\partial L}{\partial c_2}, \dots, \frac{\partial L}{\partial c_n})^T$, and similar for $\frac{\partial F}{\partial \vec{c}}$. It's also easy to verify that $W'(\phi) = 2K(\phi)K'(\phi)$.

We use the following general sequential algorithm to solve our minimization problem (3.7).

Algorithm 1. Choose initial values for ϕ and \vec{c} . For $k = 1, 2, \dots$, do

1. Find \vec{c}^{k+1} , such that

$$\vec{c}^{k+1} = \arg \min_{\vec{c}} L(\vec{c}, \phi^k). \quad (4.4)$$

2. Find ϕ^{k+1} such that

$$\phi^{k+1} = \arg \min_{\phi} L(\vec{c}^{k+1}, \phi). \quad (4.5)$$

3. Check the convergence, if converged, stop; else goto 1.

Here we use *arg min* to denote the minimizer of the functional at hand. To find a minimizer of L with respect to ϕ and \vec{c} , we need to solve

$$\frac{\partial L}{\partial \phi} = \frac{\partial F}{\partial \phi} + \frac{1}{2\mu} W'(\phi) = 0, \quad (4.6)$$

$$\frac{\partial L}{\partial \vec{c}} = 0. \quad (4.7)$$

To solve (4.6), we solve the following equation to steady state

$$\phi_t + \frac{\partial L}{\partial \phi} = \phi_t + \frac{\partial F}{\partial \phi} + \frac{1}{2\mu} W'(\phi) = 0.$$

Normally, explicit schemes are used to solve the above equation. Here, we use the Operator-splitting scheme of [25, 26] which normally has better efficiency and stability.

$$\frac{\phi^{k+1/2} - \phi^k}{\tau} + \frac{\partial F}{\partial \phi}(\phi^{k+1/2}, \vec{c}^{k+1}) = 0, \quad (4.8)$$

$$\frac{\phi^{k+1} - \phi^{k+1/2}}{\tau} + \frac{1}{\mu} K(\phi^{k+1}) K'(\phi^{k+1}) = 0. \quad (4.9)$$

To simplify the computation, we use an explicit scheme to solve (4.8),

$$\phi^{k+1/2} = \phi^k - \alpha_1 \frac{\partial F}{\partial \phi}(\phi^k, \vec{c}^{k+1}), \quad (4.10)$$

where α_1 is a constant that needs to be chosen properly. We rewrite (4.9) as

$$\phi^{k+1} - \phi^{k+1/2} + \alpha_2 K(\phi^{k+1}) K'(\phi^{k+1}) = 0, \quad (4.11)$$

where α_2 is a parameter to control the strength of the constraint. Note that (4.11) is a polynomial of ϕ^{k+1} , we use Newton method to solve it. When applying the operator-splitting scheme, we need to choose τ and μ . By transforming the algorithm into this form, we need only to choose the parameters α_1, α_2 properly.

Now we can write **Algorithm 1** more specifically as

Algorithm 2. Choose initial values for ϕ and \vec{c} . For $k = 1, 2, \dots$, do

1. Find \vec{c}^{k+1} such that

$$\vec{c}^{k+1} = \arg \min_{\vec{c}} L(\vec{c}, \phi^k).$$

2. Compute $\phi^{k+1/2}$ by

$$\phi^{k+1/2} = \phi^k - \alpha_1 \frac{\partial F}{\partial \phi}(\vec{c}^{k+1}, \phi^k),$$

3. Set $\phi^{k+1/2} = \phi^{k+1/2}$, Compute ϕ^{k+1} from solving (4.11) by Newton method.
4. Check convergence, if converged, stop; else goto 1.

4.1. Implementation Issues

- We need to choose a proper value for α_2 for the constraint equation. In order to guarantee that (4.11) has only one real root, the value of α_2 needs to be chosen according to the number n . We need to have $\alpha_2 \leq 2$ for 2 regions, and $\alpha_2 \leq 0.71$ for 3 regions. In our computations, we use $\alpha_2 = 0.01$ or 0.02 . Additionally, we don't solve the constraint equation for the first 200 iterations.
- We use fixed step size for updating both ϕ and \vec{c} . When updating ϕ , we first use a large step size $\alpha_1 = 0.1$, and change it to 0.01 after 100 iterations. When updating the constants \vec{c} , we apply the following technique:

$$\vec{c}^{k+1} = \vec{c}^k - 0.001 * \text{sign}\left(\frac{\partial L}{\partial \vec{c}}\right)(\vec{c}^k, \phi^k). \quad (4.12)$$

We found that a reasonable estimate for the constants is necessary for our algorithm to converge. Otherwise, the solution is not unique. In our numerical implementations, we define intervals $[a_j, b_j]$ for c_j and check if c_j falls out of its interval after each updating of c_j . If $c_j < a_j$, then let $c_j = a_j$; if $c_j > b_j$, then let $c_j = b_j$. The interval is chosen such that the true value sits on the center. The length of the intervals are about 30% - 50% of the difference between the true values of the constant permeability regions. In practice, it's not necessary to choose the intervals in this way. We just need to estimate the real constants and choose reasonable intervals.

5. Numerical Experiments

We will present some numerical examples to study the performance of our method. All the examples are synthetic cases, and the true permeability field consists of distinct permeability values. The test reservoir is square and horizontal with constant thickness and zero-flow outer boundaries. The fluid and rock properties are held fixed except for the absolute permeability, which is to be identified. In the field, we have one injector positioned in the lower left corner.

The relative permeability functions are defined by the Corey models

$$\kappa_{rw} = \hat{\kappa}_{rw} \left(\frac{S_w - S_{wr}}{1 - S_{wr} - S_{or}} \right)^{e_w}, \quad (5.1)$$

$$\kappa_{ro} = \hat{\kappa}_{ro} \left(\frac{S_o - S_{or}}{1 - S_{or} - S_{wr}} \right)^{e_o}, \quad (5.2)$$

where the Corey exponents, e_w and e_o , the residual saturations, S_{wr} and S_{or} , and the endpoint permeability, $\hat{\kappa}_{rw}$ and $\hat{\kappa}_{ow}$, are assumed known. The numerical values for these properties, together with the rest of the properties for the simulations, are listed in Table 5.1.

Reservoir dimensions:	1000 × 1000 × 40 meter
Simulation grid	16 × 16 × 1 cells
Porosity:	0.2
Viscosity:	$\mu_w = 0.5 \times 10^{-3}$ Pa·s, $\mu_o = \mu_w$
Endpoint relative permeability:	$\hat{k}_{rw} = 0.1, \hat{k}_{ro} = 1$
Residual saturations:	$S_{rw} = 0.2, S_{or}^* = 0.2$
Corey exponents:	$e_w = 1.5, e_o = 2.5$
Initial saturation:	$S_w = 0.2, S_o = 0.8$
Capillary pressure function:	$P_c(S_w) \equiv 0$ kPa
Injection rate:	8% of total pore volume per year
Production constraint:	constant BHP = 200.0 bar
Number of timesteps:	192
Total production time:	3000 days
Number of seismic surveys:	16

Table 5.1: Properties for the simulations.

Pressure	$\sigma_{p,well} = 1.0$ bar	$\sigma_{p,seis} = 2.5$ bar
Saturation	$\sigma_{S,well} = 0.025$	$\sigma_{S,seis} = 0.05$

Table 5.2: Standard deviations for the added noise.

For a given permeability field, we calculate the true values of pressure and saturation on the given grid. The timesteps are determined by the forward simulation. The synthetic measurements are constructed by adding noise to the calculated true values. The noise is assumed to be uncorrelated Gaussian noise with zero mean. In Table 5.2, the standard deviations, which give the amount of added noise, are listed. Notice that uncertainties are different for the seismic measurements and the production data from wells.

When incorporating these two kinds of data into the output-least-squared minimization problem, we will weight them according to the different noise levels. This is done by constructing the diagonal matrices D_{well} and D_{seis} .

To measure the data fit, we plot RMS values of J , J_{well} , and J_{seis} versus the iteration number. The *RMS* value of a function J_α is defined as $\sqrt{2J_\alpha/n_\alpha}$, where n_α is the number of measurements included in J_α and $\alpha = tot, well$ or $seis$.

We take $\vec{c} = (0, 0.3)^T$ for 2 subregion cases. and $\vec{c} = (0, 0.3, 0.7)^T$ for 3 subregion cases.

Example 1: 2 subregions, two channels

The two channels have the same higher permeability value and cross each other. This is shown in Figure 5.1.

The estimated q^k are shown in Figure 5.2. We see that, even with complicated geometrical structure, our method can recover it well after about 300 iterations. The convergence curves are plotted in Figure 5.3. Notice that, one of the constants doesn't converge well.

In this example, we take the initial value $\phi^0 = 1.5$. We have noticed that, if taking $\phi^0 = 1$, then we will miss two subchannels, and can only identify the channel running from the bottom left corner to the upper right corner. This is actually the field with relative rich flow activities. If we look at Figure 5.2(c), it's easy to find out that the permeability field with rich flow activities converges very fast, while the field with less flow activities converges much slower. This is again

a very common feature of permeability estimation problem.

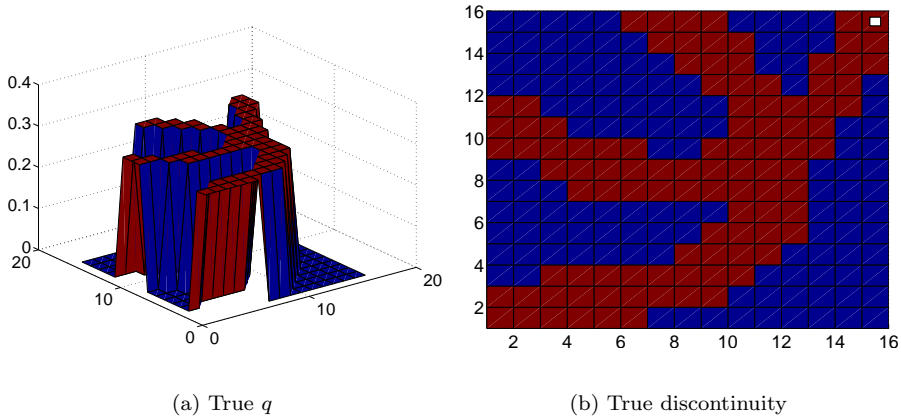


Fig. 5.1. Example 1: Two regions, multiple channels, 2 wells

Example 2: 3 subregions, single Channel

The true permeability field consists of three regions with different constant permeability values. The permeability in the channel is higher than other parts, and the channel itself consists of two parts. From near the center, the channel breaks into two parts, the part from the center to the upper right corner, has higher permeability value than the other part. The constant values for this example are $\{0, 0.3, 0.7\}$. This is shown in Figure 5.4.

The estimated q^k are shown in Figure 5.5. Convergence is achieved after about 300 iterations. Notice that some parts of the field are misclassified. Nevertheless, the basic structure is still identified well.

The convergence curves are plotted in Figure 5.6. Notice that, one of the constants refused to converge. For this test, we take the initial value $\phi^0 = 1$.

6. Conclusion and remarks

In this paper, we try to identify piecewise constant permeability fields by using a piecewise constant level set method. Numerical experiments are performed to show how our method works for two or three constant permeability regions.

Low sensitivity regions exist because of less flow activities. This makes the initial values for the level set function important for identifying these regions. For two constant permeability regions, we can naturally choose $\phi = 1.5$ as the initial guess (or $\phi = 0$ for binary level set method), together with the constraint, we can capture the low sensitivity regions without too much difficulties. However, for more than two constant permeability regions, it is difficult to choose a good initial value for ϕ . Further research needs to be done regarding this problem.

In the numerical experiments, we tried to choose the parameters (β, μ, α_i) in a consistent and systematic way. Better results could be arrived by tuning the parameters for each specific problem.

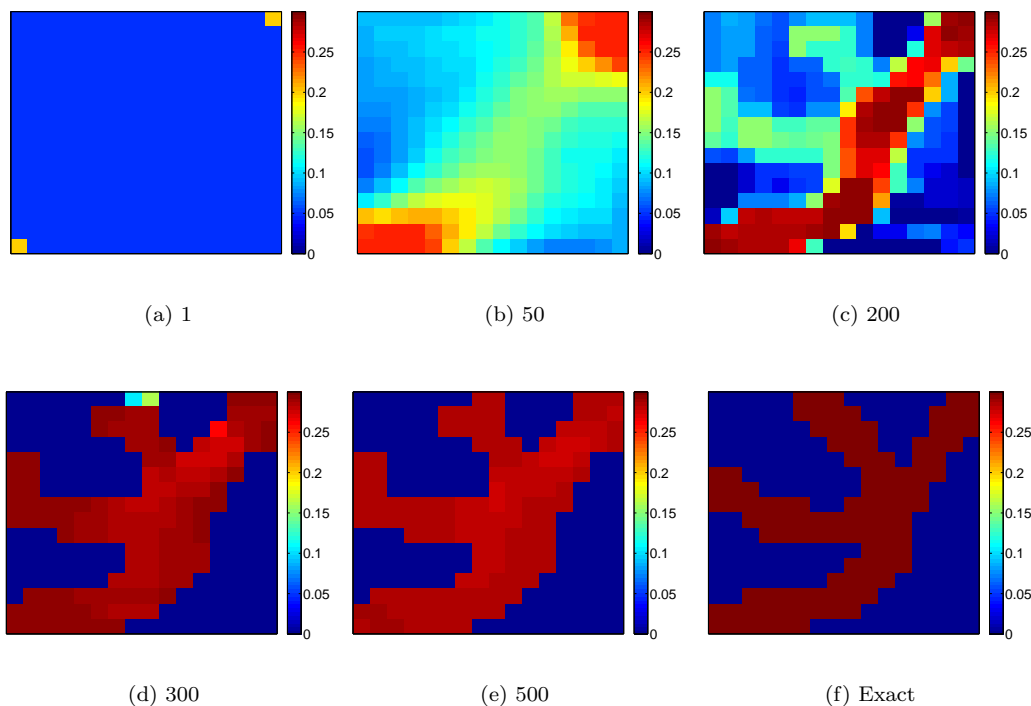


Fig. 5.2. Example 1: multiple channels, 2 wells.

Acknowledgments. This work was financed by the Norwegian Research Council, Petromaks Programme. We thank Daniel Christopher Doublet and Raymond Martinsen for providing the codes for the forward reservoir simulator and gradient calculations.

References

- [1] T. Chan and X.C. Tai, Identification of discontinuous coefficients from elliptic problems using total variation regularization, *SIAM J. Sci. Comput.*, **25** (2003), 881–904.
- [2] S. Osher and J. Sethian, Fronts propagating with curvature dependent speed: Algorithms based on hamilton-jacobi formulations, *J. Comput. Phys.*, **79** (1988), 12–49.
- [3] M. Burger, A level set method for inverse problems, *Inverse problems*, **17** (2001), 1327–1355.
- [4] K. Ito, K. Kunisch and Z. Li, Level-set function approach to an inverse interface problem, *Inverse problems*, **17** (2001), 1225–1242.
- [5] U. Ascher and E. Haber, Computational methods for large distributed parameter estimation problems with possible discontinuities, *Symp. Inverse Problems, Design and Optimization*, (2004).
- [6] R. Villegas, O. Dorn, M. Kindelan and M. Moscoso, Imaging low sensitivity regions in petroleum reservoirs using topological perturbations and level sets, *Journal of Inverse and Ill-posed Problems*, **15:2** (2007), 199–223.
- [7] R. Villegas, O. Dorn, M. Moscoso, M. Kindelan and F. Mustieles, Simultaneous characterization of geological shapes and permeability distributions in reservoirs using the level set method, paper *spe* 100291, Proc. SPE Europec/EAGE Annual Conference and Exhibition, pages 1–12, Vienna, Austria, June 12-15, 2006.
- [8] J. Lie, M. Lysaker and X.C. Tai, A variant of the level set method and applications to image segmentation, *Math. Comp.*, **75:255** (2006), 1155–1174 (electronic).

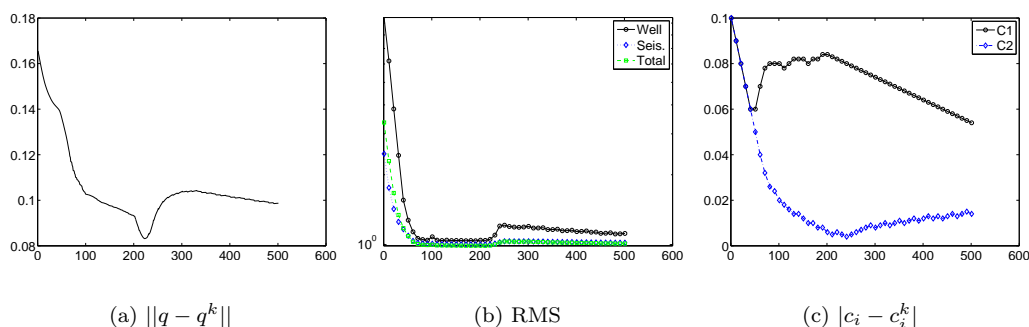


Fig. 5.3. Convergence curves for Example 1. (a) The error $\|q - q^k\|_2$. (b) The curves show the RMS values of J_{tot} , J_{well} and J_{seis} respectively. (c) The constants error.

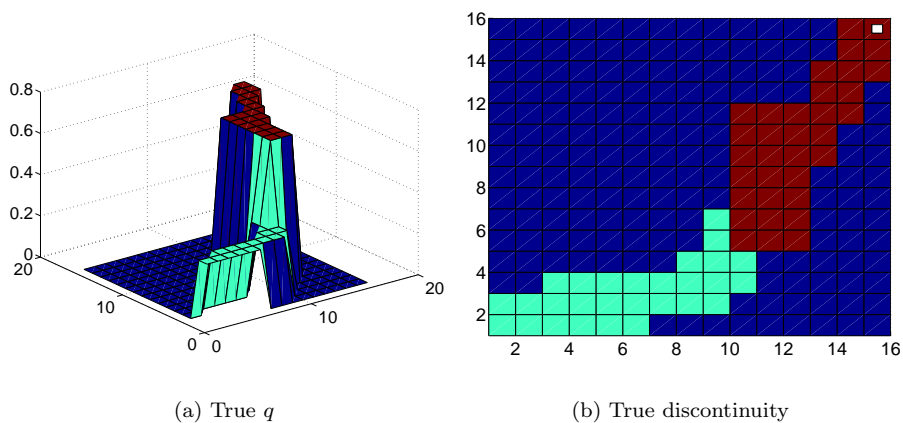


Fig. 5.4. Example 2: 3 subregions, single channel.

- [9] J. Lie, M. Lysaker and X.C. Tai, A binary level set model and some applications to mumford-shah image segmentation, *IEEE Trans. Image Process.*, **15:5** (2006), 1171–1181.
- [10] B. Song and T. Chan, A fast algorithm for level set based optimization, Technical report, Cam-report-02-68, UCLA, Applied Mathematics, 2002.
- [11] L. Nielsen, X.C. Tai, S. Aanonsen and M. Espedal, Reservoir description using a binary level set model, Image Processing based on partial differential equations, Heidelberg, 2006, Springer.
- [12] X.C. Tai and T.F. Chan, A survey on multiple level set methods with some applications for identifying piecewise constant functions, *International J. Numer. Anal. Modelling*, **1** (2004).
- [13] L.A. Vese and T.F. Chan, A multiphase level set framework for image segmentation using the mumford and shah model, *International Journal of Computer Vision*, **50:3** (2002), 271–293.
- [14] T. Chan and X.C. Tai, Level set and total variation regularization for elliptic inverse problems with discontinuous coefficients, *Journal of Computational Physics*, **193** (2003), 40–66.
- [15] J. Waggoner, A. Cominelli, R. Seymour and A. Stradiotti, Improved reservoir modelling with time-lapse seismic data in a gulf of mexico gas condensate reservoir, *Petroleum Geoscience*, **9:1** (2003), 61–72.
- [16] O. Gosselin, S. van den Berg and A. Cominelli, Integrated history-matching of production and 4d seismic data, paper *spe* 71599, Proc. SPE Annual Technical Conference and Exhibition, New Orleans, Louisiana, Oct. 2001.

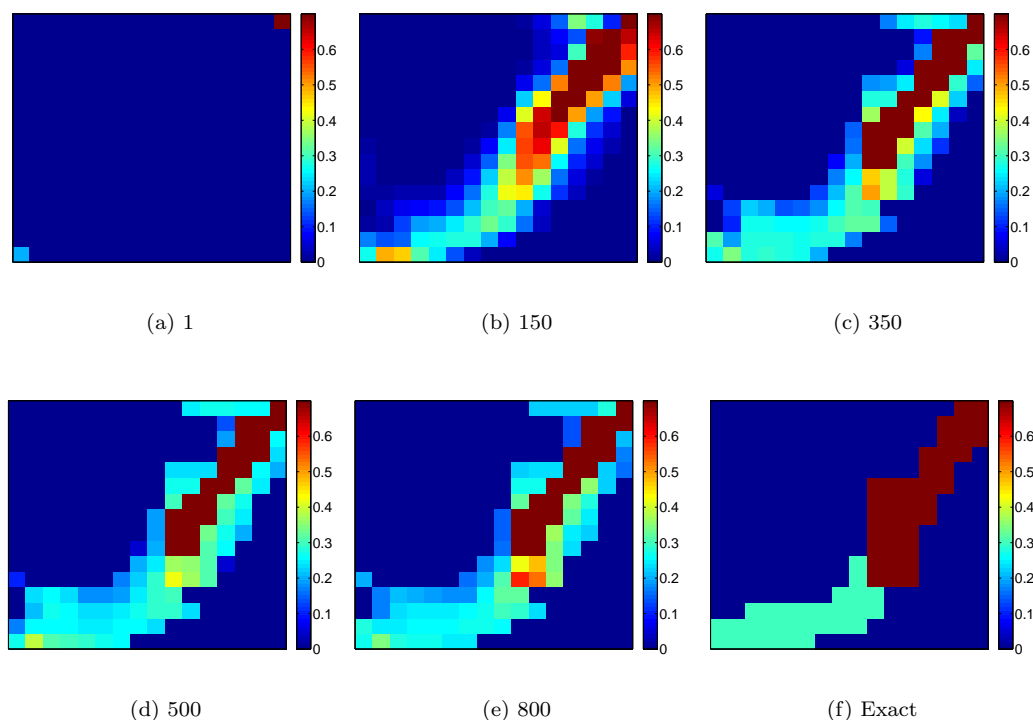


Fig. 5.5. Example 2: 3 subregions, single channel.

- [17] Y. Dong and D.S. Oliver, Quantitative use of 4d seismic data for reservoir description, *SPE Journal*, **10:1** (2005), 91–99.
- [18] S. Aanonsen, A. Cominelli, O. Gosselin, I. Aavatsmark and T. Barkve, Integration of 4d data in the history match loop by investigating scale dependent correlations in the acoustic impedance cube, Proc. 8th European Conference on the Mathematics of Oil Recovery, Freiberg, Germany, 3-6 Sept. 2002.
- [19] S. Aanonsen, I. Aavatsmark, T. Barkve, A. Cominelli, R. Gonrad, O. Gosselin, M. Kolasinski and H. Reme, Effect of scale dependent data correlations in an integrated history matching loop combining production data and 4d seismic data, paper *spe* 79665, Proc. SPE Reservoir Simulation Symposium, Houston, Texas, Feb. 2003.
- [20] M. Landrø, H.H. Veire, K. Duffaut and N. Najjar, Discrimination between pressure and fluid saturation changes from marine multicomponent time-lapse seismic data, *Geophysics*, **68** (2003), 1592–1599.
- [21] O. Kirstetter, P. Corbett, J. Sommerville and C. MacBeth, Elasticity/saturation relationships using flow simulation from an outcrop analogue for 4d seismic modelling, *Petroleum Geoscience*, **12:3** (2006), 205–219.
- [22] A. Buland and Y. Ouair, Bayesian time-lapse inversion, *Geophysics*, **71:3** (2006), R43–R48.
- [23] Y. Ouair and L. Strønen, Value creation from 4d seismic at the gullfaks field: achievements and new challenges, extended abstract, Proc. SEG Annual Meeting, New Orleans, Louisiana, October 2006.
- [24] R. Li, A. Reynolds and D. Oliver, History matching of three-phase flow production data, *SPE Journal*, **8:4** (2003), 328–340.
- [25] K. Kunisch and X.C. Tai, Sequential and parallel splitting methods for bilinear control problems in hilbertspaces, *SIAM J. Numer. Anal.*, **34** (1997), 91–118.

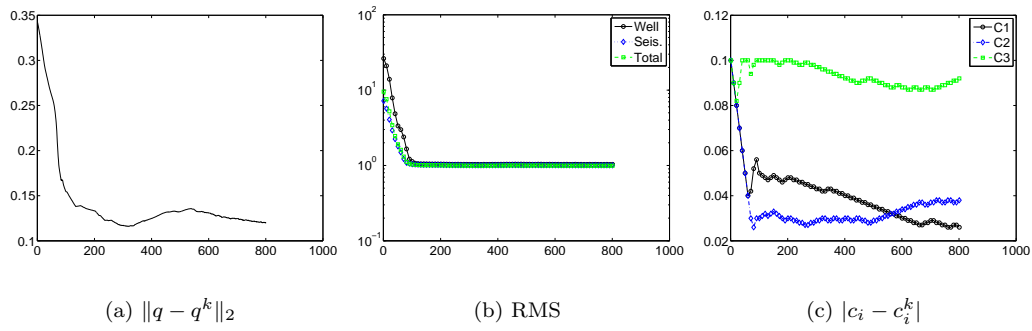


Fig. 5.6. Convergence curves for Example 2. (a) The error $\|q - q^k\|_2$. (b) The curves show the RMS values of J_{tot} , J_{well} and J_{seis} respectively. (c) The constant error.

- [26] X.C. Tai and P. Neittaanmäki, Parallel finite element splitting-up method for parabolic problems, *Numer. Methods Partial Differential Equations*, **7:3** (1991), 209–225.